Clays and Clay Minerals, Vol. 42, No. 5, 614–627, 1994.

THE SOL CONCENTRATION EFFECT IN n-BUTYLAMMONIUM VERMICULITE SWELLING

G. D. WILLIAMS, K. R. MOODY

Physical Chemistry Laboratory, South Parks Road
Oxford, OX1 3QZ, United Kingdom

M. V. SMALLEY[1]

Polymer Phasing Project, ERATO, JRDC, Keihanna Plaza
1-7 Hikari-dai, Seika-cho, Kyoto 619-02, Japan

S. M. KING

ISIS Science Division, Rutherford Appleton Laboratory
Chilton, Didcot, Oxon, OX11 0QX, United Kingdom

Abstract—The swelling of n-butylammonium vermiculite in water was investigated as a function of the sol concentration (r), the salt concentration (c) and the temperature (T).

The interlayer spacing in the gel phase was investigated as a function of r and c by neutron diffraction and by laboratory experiments which measured how many times its own volume a crystal would absorb. The salt concentration was found to be the stronger variable with the interlayer spacing decreasing proportional to $c^{0.5}$, which is consistent with previous results and with the Coulombic attraction theory. The sol concentration was found to affect the swelling for two reasons, the salt fractionation effect and the trapped salt effect. Both of these cause the salt concentration in the supernatant fluid to be greater than that originally added to the crystals and so reduce the swelling.

A new method was used for extracting the solution from inside the gels by collapsing the gels by the addition of potassium hydrogen carbonate. The Volhardt titration was carried out on the extracted and supernatant solutions from about 250 gels. The ratio of the external to the internal chloride concentration was found to be approximately constant across the range of salt concentrations. Its average value was equal to 2.6, again in agreement with Coulombic attraction theory and showing the surface potential to be constant at about 70 mV.

The (r, c, T) boundary of the two phase colloid region was investigated by three methods. A plot of log c against T_c was linear within experimental accuracy, with a gradient of 0.077 K^{-1} or 13 K per log unit. This shows that the surface potential varies by only 1 mV per decade in the salt concentration. The system is therefore governed by the Dirichlet boundary condition and not by the Nernst equation.

Key Words—CAT, DLVO theory, Neutron diffraction, Osmotic swelling, Phase transitions, Salt fractionation, Trapped salt, Vermiculite gels.

INTRODUCTION

The phenomenon of osmotic swelling only occurs with vermiculites containing certain cations. It was first observed by Walker (1960) for butylammonium vermiculites, but has also been observed by Garrett and Walker (1962) for other short chain alkyl ammonium vermiculites and more recently by Rausell-Colom *et al.* (1989) for ornithine ($H_2N\{CH_2\}_3CH\{NH_2\}CO_2H$) vermiculites. The work presented in this paper investigates the uniaxial swelling in water of n-butylammonium vermiculite. The swelling involves the absorption of large amounts of water by vermiculite crystals placed in water, leading to the interlayer spacing increasing to anything up to about 900 Å, a sufficiently large spacing for the gels to act as 1-dimensional colloids. The gels show no tendency to disperse into the surrounding solution and the neutron diffraction experiments of Braganza *et al.* (1990) have shown that the plates retain their orientation to a high degree in the swollen (gel) phase. This confirmed the results of an earlier X-ray study by Norrish and Rausell-Colom (1963) which showed sharp diffraction peaks for d-values in the range 80–300 Å.

The interlayer spacing in a vermiculite gel is determined principally by the salt concentration (salt should now be assumed to refer to n-butylammonium chloride); as the salt concentration increases the plate spacing decreases. The extreme results of Crawford *et al.* (1991) reveal that a gel in a 10^{-3} M solution has a plate spacing of around 600 Å while in a 0.1 M solution it is around 100 Å. No swelling has been observed with a salt concentration greater than 0.2 M. At higher concentrations the gel phase becomes unstable and will

[1] To whom correspondence should be addressed.

Copyright © 1994, The Clay Minerals Society

https://doi.org/10.1346/CCMN.1994.0420514 Published online by Cambridge University Press

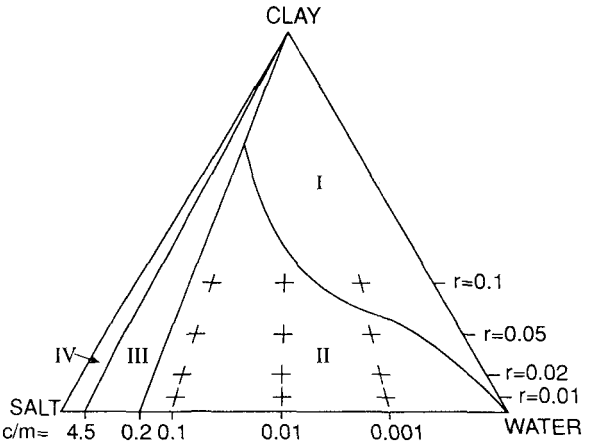


Figure 1. Phase diagram of the three component system of clay (n-butylammonium vermiculite), salt (n-butylammonium chloride) and water at constant T and P. The solid lines illustrate qualitatively the phase boundaries at T = 4°C, P = 1 atm. The left-hand wedge (region IV) represents a three phase region of crystalline clay, solid salt and saturated salt solution and the central wedge (region III) represents a two phase region of crystalline clay and salt solution. Regions I and II are the one phase (I) and two phase (II) regions of colloid stability. The crosses mark the points studied in the neutron diffraction experiments.

collapse back to a crystalline phase with a d-value of 19.4 Å if sufficient salt is added. Braganza *et al.* (1990) showed that the osmotic swelling will only occur below a critical transition temperature, T_c, that is concentration dependent. If the temperature of a swollen sample is increased above T_c it will also collapse back to the crystalline phase. The collapsed gels do not return to their original state, however; re-crystallisation occurs locally to form regions of silicate layers with a d-value of 19.4 Å. These regions are sufficiently large to give rise to a sharp diffraction pattern. The phase transition occurs within a maximum range of 2°C and was found to be completely reversible.

The sol concentration of a gel also affects swelling. The sol concentration (or volume fraction) is defined as the ratio of the volume of vermiculite to the volume of water used to prepare a gel and is denoted by r. The experiments by Braganza *et al.* (1990) were for $r < 0.01$. The experiments in this paper use four different sol concentrations, r = 0.01, 0.02, 0.05 and 0.10. The amount of water available to a gel does not directly affect swelling, except in dilute salt solutions for the case of r = 0.10 when there is insufficient water available for full swelling to occur. However, the sol concentration affects the salt concentration for two reasons. Firstly, the results presented later show that chloride ion exclusion from the region inside the gel by the negative charge on the plates leads to the salt concentration in the supernatant fluid being 2.6 times the average concentration inside the gel. As a result the sol concentration has a feedback effect on the swelling: the actual salt concentration in the solution around a gel will be greater than the original concentration due to excluded salt, so adding more solution reduces the salt concentration and therefore increases the swelling. Secondly, an unfortunate experimental feature of the vermiculite samples is that they inevitably contain a certain amount of salt in addition to any added in solution. This arises because the samples are prepared by soaking in molar solutions. The samples were mostly washed before use, normally 20 washes in demineralised water at 80°C, but there was always some salt left in the crystals. This creates a second feedback effect from the sol concentration because the salt in the crystal is diluted to a varying extent depending on the volume fraction.

N-butylammonium vermiculite in aqueous solutions of n-butylammonium chloride forms a three component system, consisting of clay, salt and water. Figure 1 illustrates qualitatively the borders between the different phases of the vermiculite.

In region III the gel phase is unstable and we have a two phase region: vermiculite crystals and solution. There is also a small three phase region (IV) of vermiculite crystals, salt crystals and saturated solution when the solubility limit of n-butylammonium chloride is exceeded (which was found by titration to be 4.5 M). The boundary of these regions is temperature dependent. Region I contains only one phase, the vermiculite gel. In this region there is not sufficient water for the gel to reach its equilibrium spacing. The boundary with region II represents the points where the gel reaches equilibrium by absorbing all the available water. Region II is the area of interest for the experiments in this paper. There are two phases, the fully swollen gel and the n-butylammonium chloride solution. Four lines show qualitatively the positions of the experiments carried out with four different volume fractions. Note that for r = 0.10 the boundary with region I prevents full osmotic swelling for lower salt concentrations.

One of the main aims of studying region II, the two-phase region of colloid stability, is to provide a test of the two theories currently used for describing the stability of colloidal systems: the established DLVO theory, developed in the 1940s by Derjaguin and Landau (1941) and independently by Verwey and Overbeek (1948), and the newer Coulombic attraction theory (CAT), proposed by Sogami (1983) and generalized by Sogami and Ise (1984).

THEORIES OF COLLOID STABILITY

The standard treatment for the interaction between charged particles in ionic colloidal solutions has for a long time been DLVO theory. This theory, which was developed independently in the 1940s by Derjaguin and Landau (1941) and Verwey and Overbeek (1948), states that the thermodynamic pair potential which

https://doi.org/10.1346/CCMN.1994.0420514 Published online by Cambridge University Press

describes the Coulombic interaction between the charged particles is a purely repulsive one. Consequently the stability of lyophobic colloids is attributed to the van der Waals attractive force.

Recently this theory has been undermined by the occurrence of discrepancies between the DLVO theory and experimental observations of clay swelling. Firstly, it has been shown by Smalley *et al.* (1989) that with n-butylammonium vermiculite the osmotically swollen gel is a true thermodynamic phase of the system, whereas DLVO theory is based on the assumption that lyophobic sols are kinetically but not thermodynamically stable. Secondly, Braganza *et al.* (1990) found no agreement between the observed interlayer separations and those predicted by DLVO theory.

Sogami and Ise (1984) have proposed a new theory regarding the electrostatic interaction in macro-ionic solutions which questions the basic assumption of DLVO theory that the Coulombic force is repulsive at all separations. They argue that the ordering observed in highly charged macro-ionic solutions is due to a long-range Coulombic attraction between the like charged particles through the intermediate counterions. Smalley (1990) has adapted this theory to the one-dimensional case, and this adaptation can be directly applied to the macro-ions of the n-butylammonium substituted vermiculite system because the silicate layers in the gel approximate well to the theoretical model of a series of parallel negatively charged plates. Assuming the plates to be perfectly parallel and of infinite size there is an electric field gradient only along the axis perpendicular to the plates, described by the 1-D Poisson equation:

$$\frac{d^2\psi}{dx^2} = \frac{\rho}{\epsilon_0}$$

where ψ is the electric potential, x is the distance from the plate, ρ is the charge density, and ϵ_0 is the permittivity.

The ion distribution is described by the Boltzmann equation and the charge density is given by

$$\rho = n_0 e[\exp\{-\Phi\} - \exp\{\Phi\}]$$

where $\Phi = e\psi/kT$, e is the electronic charge, k is Boltzmann's constant, T is the temperature, and n_0 is the number density far from the plates. Therefore,

$$\frac{d^2\psi}{d^2x} = \frac{n_0 e}{\epsilon_0}[\exp\{-\Phi\} - \exp\{\Phi\}]$$

which is the non-linear Poisson–Boltzmann equation. It can be linearised by the Debye approximation, expanding the exponentials, assuming $e\langle\psi\rangle/kT \ll 1$, where $\langle\psi\rangle$ is the mean electric potential in the gel. In fact, Crawford *et al.* (1991) have shown that at 25°C, $e\langle\psi\rangle/kT \sim 1$ for the n-butylammonium vermiculite gels, but the calculations of Sogami *et al.* (1991, 1992) involved in the non-linear model are so complicated that the linear approximation is used here. This reduces the full equation to

$$\frac{d^2\psi}{dx^2} = K\psi$$

where K is a constant, which has the physical solution

$$\psi = \psi_0 \exp\{-\kappa x\} \quad (1)$$

where $\kappa^2 = K$.

Gathering together the constants which make up K for water at 25°C, we can express it in terms of the salt concentration, c, as

$$\kappa^2 = 0.107c \quad (2)$$

where $1/\kappa$ is the Debye screening length, expressed in Å, and c is in units of mol/liter.

The electric potential described by Eq. (1) can be used to calculate the internal energy of the system, E, for any value of the interplate separation, X, by using the adiabatic approximation. The free energy of the system can then be calculated as F = E − TS or G = H − TS where H = E + PV, F is the Helmholtz free energy at constant volume and G is the Gibbs free energy at constant pressure. The graphs of the X-dependent parts of E, F and G against X are shown in Figure 2.

The Helmholtz pair potential U^F is given by

$$U^F = (8\pi e^2/\epsilon)(Z^2/\kappa)\exp(-\kappa X) \quad (3)$$

where Z is the plate valency (number of charges per unit area). Smalley (1990) has shown this to be equivalent to the repulsive potential V_R obtained by Verwey and Overbeek in the Debye limit: DLVO theory uses the Helmholtz free energy of the system assuming that the volume of the system is constant. Since the Helmholtz free energy curve has no minimum it alone would predict that the plates would spread out as far as possible. DLVO theory argues that there is also an attractive potential, V_A, arising from van der Waals forces between the plates. Taking into account retardation effects, this is given by

$$V_A = A_h/X^3 \quad (4)$$

where A_h is the Hamaker constant and is independent of the salt concentration.

At close distances the attractive force predominates, and when combined with the Born repulsion results in a deep primary minimum in the potential energy curve. In this region the strong attraction causes aggregation of the colloidal particles and results, in the case of vermiculite, in an unswollen crystalline phase. At larger distances the energy of electrical repulsion falls off more rapidly with increasing distance of separation than the van der Waals attraction, and a secondary

https://doi.org/10.1346/CCMN.1994.0420514 Published online by Cambridge University Press

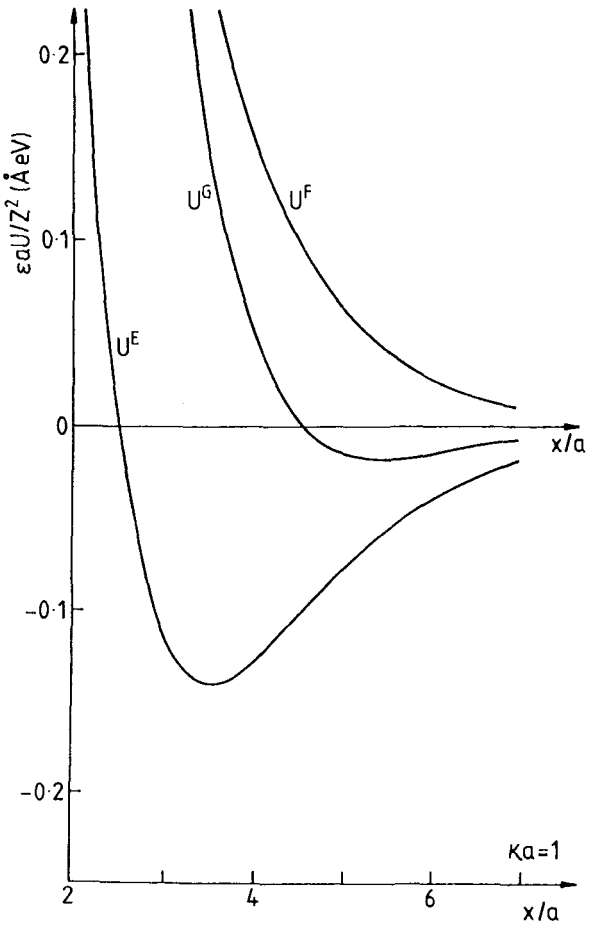


Figure 2. Comparison of the three pair potentials in the reduced forms $U^{\alpha} = \{\epsilon U^{\alpha}(X)\}/(2\pi e^2 Z^2 a)$ (α = E, F, G) for $\kappa a = 1$, where Z is the plate valency and 2a is the plate thickness, from Smalley (1990). E labels the electrostatic energy pair potential and F and G label the Helmholtz and Gibbs free energy pair potentials, respectively.

minimum occurs. This identifies with the osmotically swollen gel state of vermiculite clay, which has a well defined interlayer separation.

In order to predict the position of the secondary minimum in DLVO theory we differentiate Eqs. (3) and (4) with respect to X, giving

$$(dV_R/dX) = B \exp(-\kappa X)$$

where B is an electrostatic constant, and

$$(dV_A/dX) = (A/X^4)$$

where A is an adjustable constant. At the experimental d-value the attractive force must equal the repulsive, so DLVO theory predicts that

$$B \exp\{-\kappa d\} = A/d^4$$

or,

$$d^4 \exp\{-\kappa d\} = \text{constant} \qquad (5)$$

Braganza *et al.* (1990) found that the best possible fit of the constant in Eq. (5) to the d-values observed in the n-butylammonium vermiculite system is equal to 4.26×10^5 Å^4.

The Coulombic attraction theory argues that DLVO theory mistakenly assumes that the system has a constant volume; the volume changes according to the plate spacing, and so the Gibbs free energy of the system must be considered rather than the Helmholtz. It can be seen from Figure 2 that there is a minimum in the Gibbs free energy and so CAT provides a purely electrostatic explanation for the well defined interlayer spacing. Van der Waals interactions between the plates will be present, but in CAT they are of a much smaller magnitude than the electrostatic interactions and give only a small correction of a few percent. Norrish and Rausell-Colom (1963) have shown that the attractive forces required are too large to be explained by van der Waals forces in the n-butylammonium vermiculite system.

In CAT the potential is given by

$$U^G = \frac{2\pi e^2}{\epsilon} Z^2 \exp(-\kappa X) \cdot \left\{[1 + \cosh(2a\kappa)]\left(\frac{3}{\kappa} - X\right) + 2a \sinh(2a\kappa)\right\} \qquad (6)$$

where 2a is the thickness of the clay plates. For dilute salt solutions, $\kappa a \ll 1$ and (6) reduces to

$$V = (B/2\kappa)\exp\{-\kappa X\}[\kappa X - 3]$$

Differentiating,

$$(dV/dX) = (B/2)\exp\{-\kappa X\}[4 - \kappa X]$$

At the minimum of the curve, $(dV/dX) = 0$, so

$$\kappa d = 4,$$

or

$$d = 4/\kappa \qquad (7)$$

Eqs. (5) and (7) are the predictions of DLVO and CAT theories for the plate spacing in a gel in terms of κ, and κ is related to the salt concentration by Eq. (2). The two theories can therefore be tested experimentally by measuring the layer spacing as a function of salt concentration. The experimental results are compared with these predictions in the discussion.

In any electrostatic theory we must expect exclusion of salt from inside the gels: because negative ions are repelled from the region around the plates there is an overall deficiency of negative ions in the region inside the gel. This results in the overall concentration of these ions being significantly larger in the solution outside the gel. The following outlines calculations by Smalley (1994) concerning this salt fractionation effect.

For a flat double layer on a negatively charged plate

https://doi.org/10.1346/CCMN.1994.0420514 Published online by Cambridge University Press

the ratio, g, of the deficit of negative ions to the total charge has been given by Klaarenbeek (1946) as

$$g = \frac{1 - \exp\{e\psi_0/2kT\}}{\exp\{e\psi_0/2kT\} - \exp\{-e\psi_0/2kT\}}$$

where ψ_0 is the surface potential. In the case of the n-butylammonium vermiculite gels ψ_0 is about 70 mV, so at room temperature g = 0.20. This drops to 0.17 when allowance is made for the finite value of the mid-plane potential. The charge density, in charges per square Ångstrom, on the plates is a function of the salt concentration, given by Crawford *et al.* (1991) as

$$\sigma = 4.26 \times 10^{-2}\kappa$$

if the surface potential is constant at 70 mV. The average number density of the charge deficit is given by

$$n_{de} = 0.17\sigma/d$$

Combining the last two equations with Eqs. (2) and (7) tells us that the number density of the deficit is proportional to the overall salt concentration. Converting the number density n_{de} into a deficit molarity c_{de} using

$$n_{de} = 6.02 \times 10^{-4} c_{de}(\text{Å}^{-3})$$

the result is

$$c_{de} = 0.64c$$

For low sol concentrations this implies that

$$s = c_{ex}/c_{gel} = 2.8 \qquad (8)$$

where c_{ex} is the concentration in the supernatant solution, c_{gel} is the average concentration inside the gel and s is defined as the ratio of these two quantities. The Coulombic attraction theory predicts that the salt concentration in the supernatant fluid should be 2.8 times the average concentration in the region between the silicate layers, irrespective of the absolute value of the salt concentration. Because the layer separation has been fixed at $(4/\kappa)$ by Eq. (7) this is a prediction arising purely from CAT, which cannot be made from standard theory. The experimental results are compared with this prediction in the discussion.

Although the vermiculite gels form a useful model of a one-dimensional colloid, it should be remembered when considering the results in this paper that the gels are not a theoretical ideal. Individual samples can vary greatly, in part due to the variation of trapped salt concentration. Gels can also be not completely homogeneous. In general, experimental results can be no more accurate than within about 10% due purely to sample variation. In no case will these results be given to more than two significant figures. What we are looking for in the results is general agreement or disagreement with theory rather than absolute accuracy.

EXPERIMENTAL

The vermiculite crystals were from Eucatex, Brazil. Crystals about 30 mm^2 in area by 1 mm thick were washed and then treated for about a year with 1 M NaCl solution at 50°C, with regular changes of solution, to produce a pure Na vermiculite, following the procedure of Garrett and Walker (1962). The completeness of the exchange was checked from the regularity of the c-axis peaks in the X-ray diffraction patterns, the c-axis spacing for the Na form being 14.9 Å. To prepare the n-butylammonium vermiculite the Na form was soaked in 1 M n-butylammonium chloride solution at 50°C, with regular changes of solution, for about a month. During this process the amount of Na displaced from the crystals was determined by atomic absorption spectroscopy and the cation exchange capacity of the mineral was found to correspond to a charge density of 1.3 monovalent cations per $O^2(OH)_4$ unit. The purity was again checked by X-ray diffraction, the c-axis spacing now being 19.4 Å. The crystals were stored in a 1 M n-butylammonium chloride solution prior to the swelling experiments.

The three main purposes of the experiments were to measure the salt fractionation factor (s), the interlayer spacing (d) and the phase transition temperature (T_c) across as wide a range of (r, c) points as possible. In previous experiments on this system, r was always small, that is, the total volume of the condensed matter system, V*, was always considerably larger than the volume occupied by the macroions, V. Defining V_m to be the volume occupied by the macroions in their crystalline state, prior to soaking in the dilute salt solutions, the sol concentration is defined experimentally by

$$r = V_m/V^*.$$

Smalley *et al.* (1989) found that V* decreases by about 0.1% when the crystals swell in a 0.1 M solution. This reduction in volume is due to the electrostriction that accompanies the swelling. It is a very small change compared to that observed in V/V_m, which in this case is equal to 600%, and in the following it is assumed that V* is constant. For the case of perfectly homogeneous swelling, the amount of solution absorbed by a crystal provides an estimate of the d-spacing by:

$$d = V/V_m$$

where V is the volume of the gel, but the neutron scattering experiments provide the sharpest information on d and T_c because they probe the microscopic structure of the gels. However, the samples used in the neutron experiments were too small to provide a reliable estimate of s. The salt fractionation factor was therefore investigated by simple volumetric and gravimetric experiments.

Prior to performing an experiment on the clay, the crystals were first washed thoroughly to remove any

https://doi.org/10.1346/CCMN.1994.0420514 Published online by Cambridge University Press

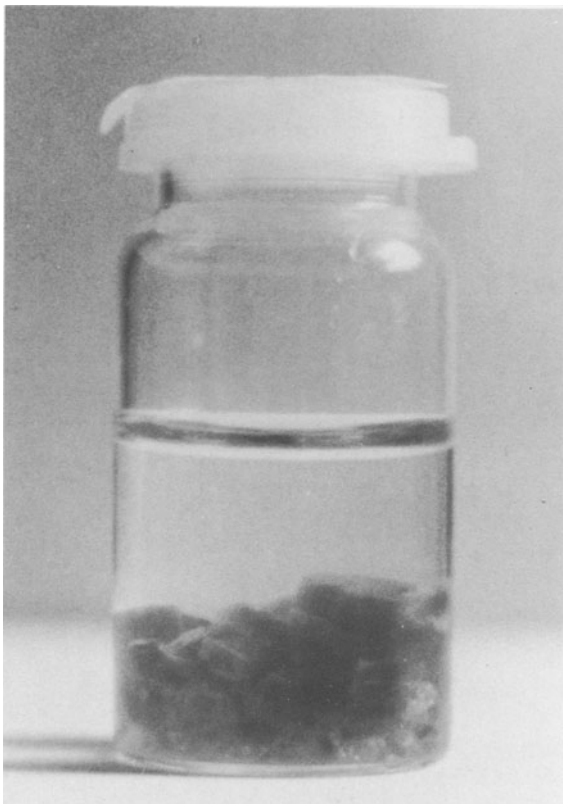


Figure 3. Photograph of a typical sample after swelling for two weeks. The height of the sample jar is approximately 5 cm.

molar solution that may be trapped in surface imperfections. This was achieved by rinsing the crystals with 500 cm^3 of distilled water at 60°–80°C twenty times before drying on filter paper. The distilled water was heated in order to prevent any swelling occurring during this washing process since, although absorption of distilled water is rapid, it does not occur above about 40°C as this is above the phase transition temperature for crystallization, as described in the results.

Even after this thorough washing procedure it was discovered that an unknown amount of salt was always present in the original vermiculite crystal. After over a year of soaking in hot molar chloride solutions in order to obtain the pure n-butylammonium form of the vermiculite, it is not surprising that the crystals, which contain cracks and pores, contain a substantial amount of n-butylammonium chloride. This salt leaches out into the solution upon swelling and so the total amount of salt present is unknown until the final concentrations in both the supernatant fluid and the gel phase and the volumes occupied by both phases have been determined.

The average density of the vermiculite crystals was found to be 1.86 ± 0.01 g cm^{-3} and the volume of vermiculite used in the experiments was determined by weighing the crystals and using this density value. In a typical experiment, approximately 0.5 cm^3 of washed and dried vermiculite crystals were accurately weighed out and their volume calculated from the density. The crystals were placed in a sealable bottle and distilled water added until the ratio of water to clay in the bottle was 50:1, that is, $50 \times V_m$ of water was added. The bottle was then sealed to prevent evaporation which would change the sol concentration, and allowed to stand for two weeks to enable the crystals to swell freely and reach equilibrium. The two week time period was not arbitrarily chosen but was determined by the kinetic experiments described by Moody (1992) and Townshend (1992). After two weeks had passed the appearance of the samples was as shown in Figure 3. While the n-butylammonium vermiculite crystals have a golden metallic sheen the gels formed by osmotic swelling are green-yellow and translucent.

After equilibrium had been reached, it was straightforward to pipette off the supernatant fluid and its concentration was easily measured by the Volhardt chloride ion titration described below. In order to measure the internal concentration, however, it was first necessary to remove the water from the gel. This proved to be more difficult. It was thought at first that this could be done by putting physical pressure on the gel. Various methods were tried but failed owing to the fragility of the gel stacks which are easily mashed into a homogeneous paste. Instead, it was decided to collapse the gels chemically by adding a salt containing a cation which inhibits swelling. Na, K, and multivalent metal cations inhibit swelling. The unhydrated K ion fits in the cavities on the plate surface and so binds the plates closely together, K Eucatex vermiculite having a plate spacing of only 10.2 Å, determined by Humes (1985). $KHCO_3$ was chosen because it is rapidly dissolved on the damp surface of the gel. This is important as it cannot be added as a solution since this would alter the chloride concentration. This method was very effective. K ions rapidly diffuse into the gel, causing it to release the interlayer fluid as a clear solution.

A small amount of $KHCO_3$ crystals were sprinkled over the gel, which was then left for 24 hours. The solution released from inside the gel was then removed by pipette. Samples of the solutions from both inside and outside the gel were then titrated for Cl^- concentration using the Volhardt titration. In the Volhardt titration for chloride ions an excess of $AgNO_3$ is added to the sample, precipitating out the Cl^- as AgCl. The remaining Ag^+ ions are then back-titrated using KSCN and a conc. $HNO_3/Fe(NO_3)_3$ indicator. At the end point, when the remaining Ag has precipitated out as AgSCN, a blood red colour is seen from the FeSCN complex formed in solution. The original chloride concentration can then be calculated. The Volhardt titration is ideal for chloride solutions of concentrations down to about 0.005 M, but below this the end point becomes in-

https://doi.org/10.1346/CCMN.1994.0420514 Published online by Cambridge University Press

creasingly harder to see accurately, so that large sets of samples were needed for each r, c point.

In the case of no added salt, the total number of moles of salt trapped inside a crystal, n_t, is given by

$$n_t = c_{ex}V_{ex} + c_{gel}V_{gel}$$

where c_{ex} and c_{gel} are the salt concentrations in the supernatant fluid and the gel phase and V_{ex} and V_{gel} are their respective volumes. Since V_m is known, the salt concentration trapped inside the crystals, c_t, was determined as

$$c_t = n_t/V_m.$$

This value was averaged over many samples studied in the laboratory and used to estimate the real salt concentration from the added salt concentration for the samples used in the neutron scattering experiments, for which the sample size was too small for the Volhard titration to be reliable.

The neutron diffraction experiments were done using the LOQ Small Angle Scattering Diffractometer at the ISIS Spallation Neutron Source, described in ISIS User Guide (1992). The LOQ instrument was chosen as it is designed for looking at spacings between 30 and 900 Å (towards the upper limit for neutrons) simultaneously and so is ideal for looking at the gels.

The experiments described by Moody (1992) and Townshend (1992) showed that for the n-butylammonium substituted vermiculite crystals to reach equilibrium in dilute n-butylammonium chloride solutions took in the region of 14 days. For this reason the samples were prepared two weeks in advance to ensure fully homogeneous swelling. The crystals were washed and dried as described previously, and after drying, the crystals were cut to dimensions of approximately 6 × 6 × 0.5 mm. These were individually weighed and the volume of the crystal in its fully hydrated state calculated using the density. Solutions of n-butylammonium chloride in D_2O were made up at concentrations of 0.1, 0.01 and 0.001 mol dm^{-3} and added to the crystals to produce the appropriate sol concentrations. The cells were sealed with parafilm for two reasons. Firstly, to prevent exchange of H_2O in the atmosphere with D_2O in the solution, and secondly, to prevent D_2O evaporating, causing a decrease in the volume of solution and an increase in the sol concentration, r.

Quartz sample cells of dimensions 1 × 1 × 5 cm were used, quartz being practically transparent to neutrons at the wavelengths utilized on LOQ. Due to the fragile nature of the swollen gels, particularly those soaked in the more dilute solutions where the extent of swelling is greatest, the vermiculite crystals were placed directly into the quartz cells after weighing and left to swell *in situ* to minimize the amount of handling required when swollen. It was necessary to swell the crystals in D_2O rather than H_2O solutions because of the large incoherent neutron scattering cross-section of hydrogen which would otherwise have obscured the scattering of interest. The small angle neutron scattering from D_2O is of low intensity and completely unstructured over the Q range used here.

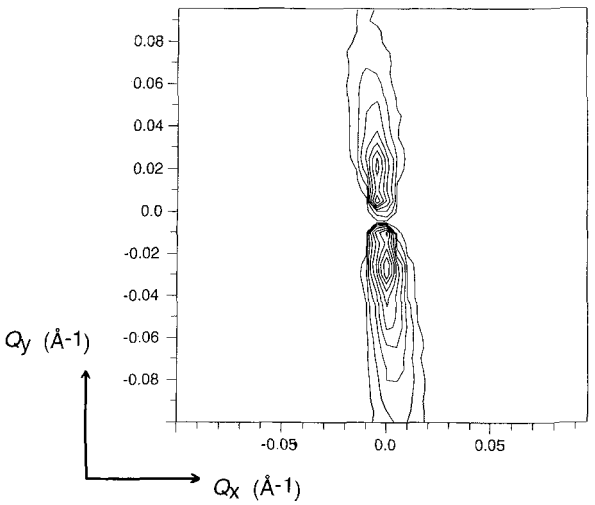


Figure 4. A contour plot of a typical neutron scattering pattern. Q_y and Q_x denote the momentum transfers ($Å^{-1}$) perpendicular and parallel to the silicate layers, respectively.

ISIS is a spallation, or pulsed, source and so time of flight instrumentation is used to measure the neutron wavelengths. This also means that the instrument can employ a "fixed" (or constant θ) scattering geometry. This in turn has the advantage that in a single run/measurement data can be collected over a wide range of Q values, where Q, the modulus of the scattering vector, is given by

$$Q = (4\pi/\lambda)\cdot\sin\theta$$

where λ is the neutron wavelength and 2θ is the scattering angle. On LOQ a wavelength limiting chopper operating at 25 Hz provides an incident neutron beam with wavelengths between 2 and 10 Å. Typically the Q-range of LOQ is 0.007 $Å^{-1}$ to 0.2 $Å^{-1}$.

Due to the parallel plate geometry of the gel samples under investigation, the incident beam was collimated by passage through a 2 × 8 mm slit placed immediately before the samples. This produced a flat beam of neutrons parallel to the clay plates rather than the 8 mm diameter circular collimation normally employed. The samples were mounted on a temperature controlled 20 position sample changer under the control of the instrument computer.

Neutrons scattered by the gel samples were recorded on a large two-dimensional "area" detector, the active area of which was 64 × 64 cm, situated approximately 4.5 m behind the samples. This was a ^3He gas detector, software coded as 64 × 64 pixels × 102 time channels. A typical scattering pattern from a gel sample (for all wavelengths) is shown in Figure 4.

https://doi.org/10.1346/CCMN.1994.0420514 Published online by Cambridge University Press

Table 1. The twelve sets of results obtained for the salt fractionation effect.

r	c/M	W	N_s	c_{ex}/mM	c_{gel}/mM	s
0.01	0	20	32	1.4 ± 0.4	0.8 ± 0.5	1.6 ± 1.5
0.01	0	0	16	3.3 ± 0.4	1.2 ± 0.3	2.7 ± 1.0
0.01	0.03	20	16	30	5	6.0
0.01	0.10	20	16	105 ± 1.8	39 ± 7.7	2.7 ± 0.6
0.02	0	20	32	1.1 ± 0.5	0.5 ± 0.3	2.2 ± 2.0
0.02	0	0	20	13 ± 2.2	8.0 ± 1.9	1.6 ± 0.7
0.02	0.03	20	16	32 ± 2.0	8.6 ± 1.1	3.7 ± 0.7
0.02	0.10	20	16	110 ± 2.5	40 ± 2.4	2.7 ± 0.2
0.05	0	20	32	11 ± 2.6	4.7 ± 1.7	2.3 ± 1.4
0.05	0	0	16	37 ± 2.4	15 ± 1.7	2.5 ± 0.4
0.05	0.03	20	16	40 ± 4.0	14 ± 1.5	2.9 ± 0.6
0.05	0.10	20	16	120 ± 2.7	38 ± 4.3	3.2 ± 0.4

r is the sol concentration, c/M is the salt concentration of the solution added to the crystals expressed as a molarity, W is the number of washes that the crystals were given and N_s the number of samples which were used under each set of conditions. c_{ex}/mM and c_{gel}/mM are, respectively, the measured salt concentrations in the supernatant fluid and the gel phase, expressed as millimolar quantities, and $s = c_{ex}/c_{gel}$ is the salt fractionation factor.

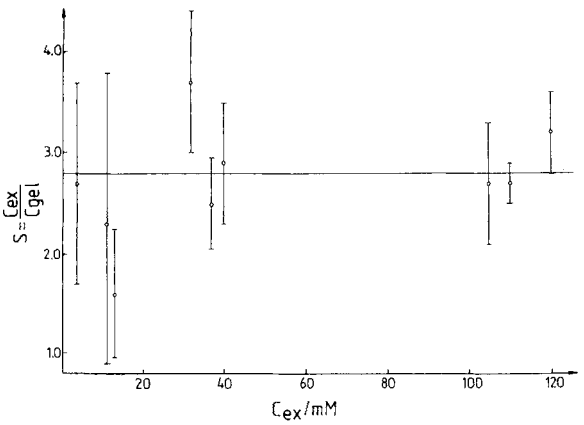


Figure 5. The salt fractionation effect in n-butylammonium vermiculite swelling. $s = c_{ex}/c_{gel}$ is plotted as a function of c_{ex}, the salt concentration in the supernatant fluid. The solid line shows the CAT prediction, s = 2.8.

Figure 4 represents the corrected data from the detector, with intensity contours plotted as a function of the scattering vector perpendicular (Q_y) and parallel (Q_x) to the layers. The scattering pattern consists of two lobes of intensity above and below the plane of the layers in the gel. If the layers were perfectly parallel then coherent scattering would only occur along the axis perpendicular to the layers, but in reality there are defects in the gel so scattering occurs either side of the axis. The width of the lobe is an indication of the parallelity of the gel stack. I(Q) against Q plots were obtained by radially summing the intensity at constant Q around the detector. At the same time the azimuthal range was limited to between 60° and 120° in order to give a more detailed diffraction pattern. All of the sample runs were corrected for the transmission (using the straight through beam) and for the background scattering using a cell containing D_2O. In this way the scattering patterns analysed arose purely from the gels.

RESULTS

Salt fractionation effect

The gels were prepared in the standard way, the crystals being washed 20 times, unless stated otherwise. Three volume fractions were investigated, r = 0.01, 0.02 and 0.05. For each volume fraction four sets of samples were investigated:

i) Crystals swollen in demineralised water.
ii) Unwashed crystals swollen in demineralised water.
iii) Crystals swollen in 0.03 M n-butylammonium chloride solution.
iv) Crystals swollen in 0.10 M n-butylammonium chloride solution.

For each set of conditions at least 16 samples were prepared to assess sample to sample variation. The crystals were left to swell for two weeks in order to ensure that they had reached equilibrium. The samples were then weighed, the solution removed by pipette, and the samples weighed again. These weighings allowed the mass of the solution to be calculated and so, knowing the initial mass of water added to the crystal, the mass of water absorbed by the crystal. This result was used to calculate the d-spacing in the gel and is discussed below. The twelve sets of results for the salt fractionation effect are given in Table 1.

The measured salt concentrations in the supernatant fluid, c_{ex}, and the gel phase, c_{gel}, have been given in the form $\mu \pm \sigma$ in Table 1, where μ is the average result and σ is its standard deviation. The exception is the r = 0.01, c = 0.03 M result, for which only the average values are given. This result was not regarded as significant because the global average of s over the 244 pairs of titrations performed was equal to 2.7, so that the result in this case, s = 6.0, lay more than three standard deviations from the mean. After this abnormal result had been discarded, the average over the remaining eleven sets of results was s = 2.6.

In each case s was determined both as the average over the N_s individual determinations of c_{ex}/c_{gel} and as the ratio $\langle c_{ex}\rangle/\langle c_{gel}\rangle$ and these two results were found to be equal to two significant figures. The range of s expressed after the ± sign in the final column of Table 1 was therefore obtained by expressing the standard deviations in c_{ex} and c_{gel} as percentages of their means, adding these two figures to give a compound percentage error and multiplying this number by the average value of s. These numbers have been plotted as the error bars

https://doi.org/10.1346/CCMN.1994.0420514 Published online by Cambridge University Press

in Figure 5, which shows s as a function of the equilibrium salt concentration in the supernatant fluid, c_{ex}.

The most obvious feature of Table 1 and Figure 5 is that there seems to be no systematic variation of s with respect to c_{ex}, in agreement with the Coulombic attraction theory. The CAT prediction, s = 2.8, which is also plotted on Figure 5, fits most of the data, there being only two points whose error bars lie outside the predicted value of 2.8, one above and one below. It should be noted, however, that the percentage compound error in s is very large at the lower salt concentrations because of the lesser accuracy of the Volhardt titration and so we would not be sensitive to deviations from the prediction for $c_{ex} < 2$ mM. The two results in this range have been omitted from Figure 5 because the percentage error in these cases approaches 100%. In the range 3 mM $< c_{ex} <$ 120 mM, we conclude that s is constant and equal to 2.6 ± 0.4.

As the salt concentrations both inside and outside the gels were measured as well as the amount of water absorbed by the gel the total amount of salt present in a sample could be calculated and so we could determine the concentration of salt trapped in the original crystals. This is an important result since without it we cannot know the salt concentration in a gel simply from the salt concentration of the solution used to prepare it. The amount of trapped salt is dependent on how thoroughly the crystals have been washed: since we are primarily interested in the amount of salt contained by crystals after the standard treatment (20 washes in demineralized water at 60°–80°C) the data for W = 0 were omitted from this determination. The data for c = 0.1 M and r = 0.01, c = 0.03 M were also omitted from this determination because the trapped salt was not seen significantly vis-a-vis the added electrolyte in these cases. The three best data sets, those with W = 20, c = 0, each obtained for 32 samples ($N_s = 32$), gave C_t = 0.04 M, 0.12 M and 0.09 M for r = 0.01, 0.02 and 0.05 respectively. The two remaining data sets determined for 16 samples ($N_s = 16$) both gave c_t = 0.15 M, so the final average result was c_t = 0.10 M. The spread of the results suggests that c_t varies between sets of crystals (in each case all of the crystals used in an experiment were washed together) and that an appropriate range to take for c_t is ±0.05 M. We therefore conclude that:

$$c_t = 0.10 \pm 0.05 \text{ M}.$$

This result is used below to calculate the real salt concentration in the samples studied in neutron scattering experiments, for which the sample size was too small for the Volhardt titration to be reliable.

Neutron diffraction study

The object of the experiments was to find the c-axis spacing, d, in the gel and the phase transition temperature, T_c, for each of 16 sets of (r, c) conditions. These were r = 0.01, 0.02, 0.05 and 0.10 for each of c = 0, 10^{-3} M, 10^{-2} M and 10^{-1} M, although the actual salt concentrations were greater due to the salt trapped in the crystals. The real salt concentrations are given in Table 2.

Table 2. The real salt concentrations (mM) in the neutron diffraction experiments and laboratory T_c experiments.

	c			
r	0 M	10^{-3} M	10^{-2} M	10^{-1} M
0.01	1 ± 0.5	2 ± 0.5	11 ± 0.5	101 ± 0.5
0.02	2 ± 1.0	3 ± 1.0	12 ± 1.0	102 ± 1.0
0.05	5 ± 2.5	6 ± 2.5	15 ± 2.5	105 ± 2.5
0.10	10 ± 5.0	11 ± 5.0	20 ± 5.0	110 ± 5.0

First, the sample changer was maintained at 2°C. For each (r, c) point four samples were made; this was necessary due to sample to sample variation and to ensure at least one of each set gave a clear peak. It was found that good statistics could be obtained in about 15 minutes. The sample giving the clearest scattering pattern was selected from each set of four and those sixteen were run at higher temperatures, increasing the temperature in 2°C steps. These temperature scans were only run for about three minutes since beam time was limited and the collapse of a gel could be seen by the disappearance of the peak, without needing the very good statistics of the earlier sets of data.

The d-values and transition temperatures calculated from the neutron experiments are tabulated below for direct comparison with results from the laboratory experiments. Samples of the diffraction patterns obtained are shown here to illustrate various features.

Figures 6(a) and 6(b) both show sets of results for four identical samples at 2°C, clearly showing the peaks from which the d-spacing in a gel is calculated. Figure 6(a) shows a set for which there is little sample to sample variation in the position of the peak. The four plots show peaks of different intensities, but this is due to physical differences in the size of the gels; the wider the section of gel in the neutron beam is, the more intense the scattering. One of the plots has a distinct second order peak, which is fairly rare. Figure 6(b) shows the sample to sample variation which can occur, in this case there being two plots giving clear peaks with different Q values as well as one which gives no peak at all. Figure 7 shows the runs for a single sample at 18°, 20° and 22°C. The traces clearly show the disappearance of the peak as the gel collapses. In this case T_c = 20° ± 1°C.

Interlayer spacings

In order to extract the most precise information from the neutron diffraction patterns it will be necessary to analyse them quantitatively using a one-dimensional paracrystalline lattice model, as described by Hashimoto *et al.* (1978). However, the sharpness of the dif-

https://doi.org/10.1346/CCMN.1994.0420514 Published online by Cambridge University Press

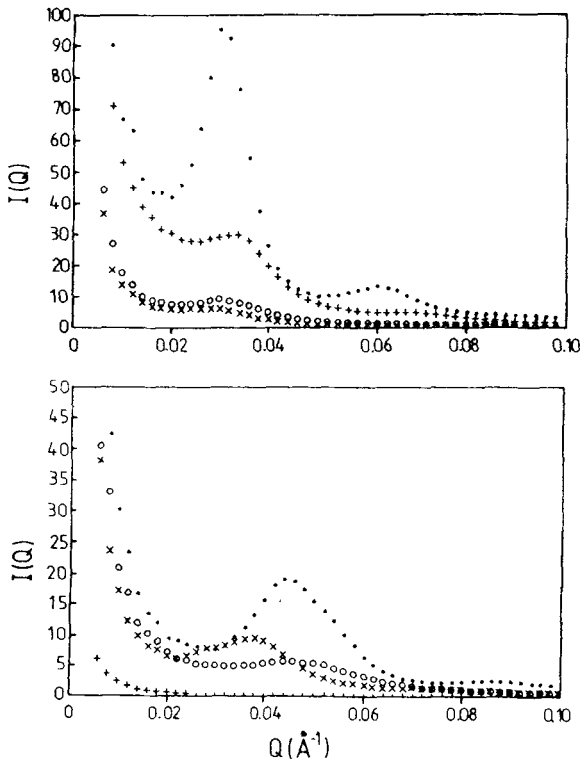


Figure 6. I(Q) (arbitrary units) vs. Q patterns obtained at 2°C for four different samples. Top shows the four traces obtained from the four different samples prepared at r = 0.05, c = 0. Bottom shows the four traces obtained at r = 0.1, c = 0.001 M.

fraction effect permits an immediate approximate evaluation of the average interplate separation by simply observing Q_{max}, the Q-value at the maximum of the first order diffraction effect, and applying the simple equation

$$d = (2\pi/Q_{max})$$

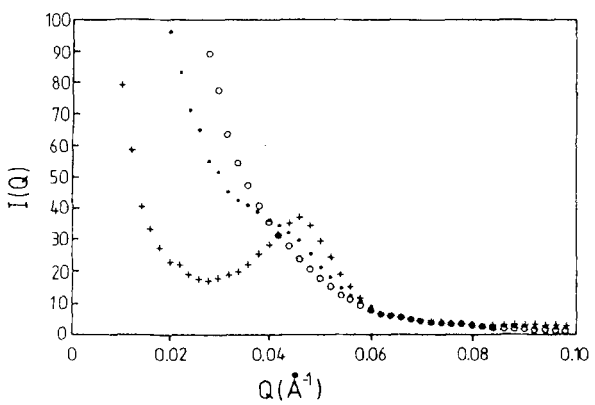


Figure 7. I(Q) vs. Q plots obtained for one sample at r = 0.1, c = 0.01 M. The crosses (+), stars (*) and circles (○) show the scans obtained at 18°, 20°, and 22°C, respectively.

Table 3. The interlayer spacing d as a function of the salt concentration c from neutron diffraction experiments.

c/M	d/Å	$dc^{0.5}/ÅM^{0.5}$	$d^4\exp\{-dc^{0.5}\}/Å^4$
0.0012	520	18	$3.0\ 10^{-2}$
0.0023	480	23	5.4
0.0027	450	23	4.2
0.0042	490	32	$7.3\ 10^{-4}$
0.0071	210	18	$3.0\ 10^{1}$
0.0085	210	19	$1.1\ 10^{1}$
0.012	310	34	$1.6\ 10^{-5}$
0.015	305	37	$7.4\ 10^{-7}$
0.016	135	17	$1.4\ 10^{1}$
0.018	150	20	1.7
0.021	200	29	$4.1\ 10^{-4}$
0.027	130	21	0.22
0.10	120	38	$6.5\ 10^{-9}$
0.11	120	40	$8.8\ 10^{-10}$
0.12	110	38	$4.6\ 10^{-9}$
0.13	95	34	$1.4\ 10^{-7}$

The quantities calculated in columns 3 and 4 are predicted to be constant by the CAT and DLVO theory respectively.

The results of this analysis are given in Table 3, where the salt concentrations have been taken from Table 2. The third and fourth columns in Table 3 have been calculated by applying the predictions of the CAT and DLVO theory given by Eqs. (10) and (9), derived in the following section.

The predictions can also be compared with the results of the soaking experiments described above in which the number of volumes of water absorbed by a single volume of crystal was measured. Because the crystal contains one layer every 19.4 Å and swelling is homogeneous, for each volume of water it absorbs the interlayer spacing must have increased by 19.4 Å. The conditions used for these gels are listed in Table 1 and the results are given in Table 4. Table 4 also lists N_s, the number of samples which were used for each set of conditions.

There is a systematic variation between the two sets of results, those from the neutron experiments giving lower layer spacings than the laboratory experiments. This could be because the samples used contained a higher than average trapped salt concentration or possibly due to the use of D_2O instead of H_2O to prepare those samples. The difference is, however, small and so both sets of results will be discussed together below.

Phase transition temperature

Experiments were carried out to investigate T_c, the temperature above which the gels become unstable, for gels prepared at sixteen (r, c) points: r = 0.01, 0.02, 0.05 and 0.10 for each of c = 0, 10^{-3} M, 10^{-2} M and 10^{-1} M. All of the samples were prepared using solutions in D_2O. This was necessary for the neutron diffraction experiments and it was decided to use D_2O in subsequent experiments so that the results could be

https://doi.org/10.1346/CCMN.1994.0420514 Published online by Cambridge University Press

Table 4. The interlayer spacing d as a function of the salt concentration c from laboratory experiments. N_s is the number of samples used in each determination.

N_s	c/M	d/Å	$dc^{0.5}/ÅM^{0.5}$	$d^4\exp\{-dc^{0.5}\}/Å^4$
32	0.0010	620	20	$3.0\ 10^{-2}$
32	0.0014	600	22	$3.6\ 10^{1}$
16	0.0033	540	31	$2.9\ 10^{-3}$
32	0.011	235	24	0.12
20	0.013	260	30	$4.2\ 10^{-4}$
16	0.030	300	52	$2.1\ 10^{-13}$
16	0.032	290	52	$1.8\ 10^{-13}$
16	0.037	240	46	$3.5\ 10^{-11}$
16	0.040	235	47	$1.2\ 10^{-11}$
16	0.105	220	71	$3.4\ 10^{-22}$
16	0.110	210	69	$2.1\ 10^{-21}$
16	0.120	195	68	$4.2\ 10^{-21}$

The quantities calculated in columns 4 and 5 are predicted to be constant by the CAT and DLVO theory respectively.

Table 5. The phase transition temperatures (°C) obtained by three methods.

r	c: 0 M	10^{-3} M	10^{-2} M	10^{-1} M
	(a) Neutron diffraction			
0.01	>34	>34	27 ± 1	13 ± 1
0.02	34 ± 1	>34	27 ± 1	12 ± 1
0.05	20 ± 1	23 ± 1	22 ± 1	9 ± 1
0.10	20 ± 2	22 ± 3	19 ± 1	9 ± 1
	(b) Laboratory cooling experiments			
0.01	37 ± 1	36 ± 2	26 ± 1	13 ± 1
0.02	33 ± 1	34 ± 1	27 ± 1	12 ± 1
0.05	31 ± 1	31 ± 1	25 ± 1	12 ± 1
0.10	27 ± 1	26 ± 1	22 ± 1	11 ± 1
	(c) Laboratory heating experiments			
0.01	>39	>39	28 ± 2	14 ± 1
0.02	36 ± 4	37 ± 3	28 ± 2	15 ± 1
0.05	34 ± 2	32 ± 2	28 ± 1	12 ± 1
0.10	26 ± 2	26 ± 2	26 ± 2	13 ± 1

directly compared without having to consider any possible isotope effect.

Three types of experiment were carried out:

i) The neutron diffraction experiments described above.

ii) A set of 16 samples were placed in a water bath at 55°C immediately after preparation so that they would not swell. The temperature of the water bath was then reduced by 1°C at 24 hour intervals and the temperature noted at which the first signs of swelling were seen.

iii) Two sets of 16 samples were placed in a water bath at 4°C and left for two weeks to swell to equilibrium. The temperature of the water bath was then increased by 1°C every 24 hours and the temperature noted at which the gels collapsed.

The results from the three sets of experiments are listed in the above order in Tables 5a, b and c, which include the approximate errors for each result.

The three sets of results are in good agreement, the variations representing an error of only a few percent in an absolute temperature of approximately 300 K. Of the three sets the neutron data are probably the most accurate since the collapse of the gel was seen very clearly by the disappearance of the diffraction peak within the range of two degrees Kelvin (Figure 7). In the second set of experiments the onset of swelling as temperature was increased could be seen fairly clearly but the third method was less accurate as it is much harder to see the exact temperature at which collapse occurs. When a gel collapses it does not regain its original crystalline appearance; groups of plates conglomerate but the structure as a whole becomes broken up and does not decrease significantly in volume. The most reliable indication of collapse is the appearance of the metallic sheen of the crystal but this too can be hard to spot and so the errors are larger in Table 5c. This method, however, was the only one for which more than one sample under each set of r, c conditions was used and so the errors in Table 5c do contain an indication of the level of sample to sample variation. This is in any case the most likely source of variation in the results rather than experimental error because of the variation in trapped salt concentration. It can be seen from Table 2 that for low c and high r conditions this error is greater than that in the values obtained for T_c and so an average over all the results will be used. The largest inconsistency is that the neutron experiments give consistently lower results than the other two methods. This suggests that the batch of crystals used for them had a higher than average concentration of trapped salt, a conclusion which is consistent with the results obtained for the d-values. The results for the second two methods are very consistent. Since they approach the phase transition from opposite sides, this shows that there are no hysteresis loops.

DISCUSSION

In the theory section it was shown how the predictions of the CAT and DLVO theory differ as regards the plate spacing inside a gel at different salt concentrations, namely

$$\text{DLVO:}\quad d^4\exp\{-\kappa d\} = \text{constant} \qquad (5)$$

$$\text{CAT:}\quad d = 4/\kappa \qquad (7)$$

$$\text{with}\quad \kappa^2 = 0.1c \qquad (2)$$

Combining (2) with each of (5) and (7) the predictions become

$$\text{DLVO:}\quad d^4\exp\{-dc^{0.5}\} = \text{constant} \qquad (9)$$

$$\text{CAT:}\quad d = 13c^{-0.5} \qquad (10)$$

where d is in Å and c is in mol liter^{-1}.

https://doi.org/10.1346/CCMN.1994.0420514 Published online by Cambridge University Press

Table 6. The modified CAT prediction with a plate thickness 2a = 19.4 Å.

c/M	$\frac{4}{\kappa}$/Å	f(a, κ)/Å	d(theory)/Å	d(exp)/Å
0.1	40	15	55	140
0.03	73	9	82	180
0.01	126	6	132	260
0.003	231	3	234	430
0.001	400	2	402	620

c is the salt concentration, $4/\kappa$ is the leading term in the CAT prediction and f(a, κ) is the correction term. The fourth column gives the modified CAT prediction and the fifth column gives the average experimental result.

Table 7. The modified CAT predictions with layer thicknesses of 30 Å and 80 Å.

c/M	$\frac{4}{\kappa}$/Å	f(a, κ) 2a = 30	f(a,κ) 2a = 80	d(2a = 30)/Å	d(2a = 80)/Å	d(exp)/Å
0.1	40	27	80	67	120	140
0.03	73	20	78	93	151	180
0.01	126	13	69	139	195	260
0.003	231	7	47	238	278	430
0.001	400	4	30	404	430	620

c is the salt concentration, $(4/\kappa)$ is the leading term in the CAT prediction and f(a, κ) is the correction term. The fifth and sixth columns give the modified CAT predictions and the seventh column gives the average experimental result.

It is very clear from Tables 3 and 4 that the prediction of DLVO theory does not fit the experimental data. In Table 3 the calculated values of $d^4\exp\{-dc^{0.5}\}$, predicted by DLVO to be a constant, vary by eleven orders of magnitude. In Table 4 there is an even greater range, the same quantity varying by 23 orders of magnitude. CAT fits the experimental results much more closely: the calculated values of $dc^{0.5}$ vary only by a factor of 2 for the neutron data and by a factor of 3 for the laboratory experiments. Although this may seem a poor approximation to a constant it must be remembered that there is a large degree of variation in the gels themselves, as they are pieces of clay rather than theoretical models. We are therefore looking for general rather than accurate agreement. The main conclusion of this section is that *CAT is consistent with the experimental results: DLVO theory is not.*

One factor which might explain some of the discrepancy between CAT and the experimental results is the thickness of the silicate layers themselves. Up to now we have approximated the interlayer spacing as the distance over which the system repeats, but this also includes a silicate layer with a bare thickness of around 10 Å and two strongly adsorbed n-butylammonium layers. This gives an insignificant correction at low salt concentrations when a gel may have a plate spacing of 600 Å, but becomes important as the spacing decreases to below 100 Å. Eq. (7) is only the small kappa prediction of CAT, the full equation being given by

$$d = \frac{1}{\kappa}\left(4 + 2a\kappa\frac{\sinh\{2a\kappa\}}{1 + \cosh\{2a\kappa\}}\right) \qquad (11)$$

where 2a is the plate thickness, as shown by Smalley (1990).

The theoretical prediction for the plate spacing now varies from the original value of four Debye screening lengths in dilute salt concentrations to over five Debye screening lengths in a 0.1 M solution. The predictions of Eq. (11) for the plate spacing at various salt concentrations are compared with the experimental results in Table 6. The parameter 2a has been taken to be 19.4 Å because this is the experimentally observed c-axis spacing in the crystal. The second term has been abbreviated to f(a, κ) in the tables.

There is still a discrepancy between the theory and the observed results. It may be possible to partly account for this by taking the idea of the silicate layer thickness a step further, as first suggested by Rausel(l)-Colom (1964). Although the distribution of butylammonium ions in the crystal has not yet been determined, a likely arrangement is that the positively charged NH_3^+ head groups will form a layer on the surface of the clay particles. Even when the crystal swells these layers are likely to persist on the surface of the particles and both adsorbed layers would have a thickness of about 9.4 Å. It may be that we ought to be considering not the spacing between the silicate layers but the spacing between the ordered regions centered around them, which by Rausell-Colom's argument are considered to be approximately 30 Å thick.

Furthermore, it could be argued that the ordered structure around the plates extends out into the solution between the plates. Various authors have suggested that there will be an ordering of the polar water molecules into layers on the clay particles. The effective layer thickness might therefore be even greater than 30 Å. A fact which may be relevant here is that it is impossible to make a two-phase gel with a plate spacing of less than about 80 Å, since at higher salt concentrations the gel collapses back to the crystal phase. Perhaps 80 Å could represent the true thickness of the ordered structure? Since a layer of water molecules takes up about 2.5 Å this would involve 20 layers of water between each silicate layer, or in other words that the ordering due to each plate must extend over 10 layers. The predicted results using layer thicknesses of 30 and 80 Å are listed in Table 7, which shows that by using a layer thickness of 80 Å CAT gives good agreement with the experimental results at high salt concentrations. Such an agreement may be fortuitous as it is unlikely that any sort of ordering could extend to ten layers of water on each plate since such a structure is at the expense of the entropy of the solution.

It is noteworthy that while spectroscopists invariably find that the clay surface influences at most the first

https://doi.org/10.1346/CCMN.1994.0420514 Published online by Cambridge University Press

two layers of water molecules, the interpretation of our data in terms of an ordered structure of 80 Å around a clay particle implies that the clay has a relatively long distance influence on its environment. This duality probably arises because the spectroscopic technique probes only the local environment of the water molecules, whereas we are measuring the long-range equilibrium properties of the gel structure as a whole. The better fit we obtain to our data with 2a = 80 Å is in agreement with the work of Low (1987), who looks at clay suspensions from a thermodynamic viewpoint. This emphasises the thermodynamic nature of our approach, a point which is particularly important in attempting to understand the nature of the phase transition between the crystalline and gel states.

The phase transition is thermodynamic, so it will occur when the primary and secondary minima are of equal depth. We might expect the free energy of the crystalline state to be relatively insensitive to temperature. In this case, variations of T_c correspond to variations in the depth of the secondary minimum, which is sensitive to the surface potential, ψ_0: the electrostatic constant B contains the square of ψ_0. The effect therefore gives us a measure of the way in which ψ_0 varies with c. The exact functional dependence of ψ_0 on T_c is unknown, but it seems reasonable to assume that the ratio of $e\psi_0/kT_c$ will remain constant along the c, T phase boundary if the behaviour of the system is dominated by electrostatic forces. As the temperature of the transition decreases with increasing salt concentration, this suggests that the magnitude of the surface potential is also decreasing with c.

If we now look for Nernstian behaviour in the system then

$$\psi = \psi_0 + (RT/zF)\ln c \qquad (12)$$

suggests that a plot of the surface potential against log c should be linear. This further suggests that a plot of T_c against log c might also be linear, and Figure 8 shows that this is indeed the case.

The T_c values in Figure 8 have been taken as the average over Tables 5a, b and c and the c values have been taken from Table 2. The gradient of the graph is $-0.077\ K^{-1}$, corresponding to a decrease of 13 K per log unit. In electrical terms that corresponds to a decrease of only 1 mV per decade of salt concentration compared to 58 mV as predicted by the Nernst equation. This shows that the n-butylammonium gels form a more or less constant surface potential system rather than a constant surface charge system and are therefore governed by the Dirichlet boundary condition rather than the Nernst equation. Smalley (1994) has shown that this conclusion agrees with the constancy of the salt fractionation effect and it agrees with that reached by Crawford *et al.* (1991) from the effect of uniaxial stress on the gels.

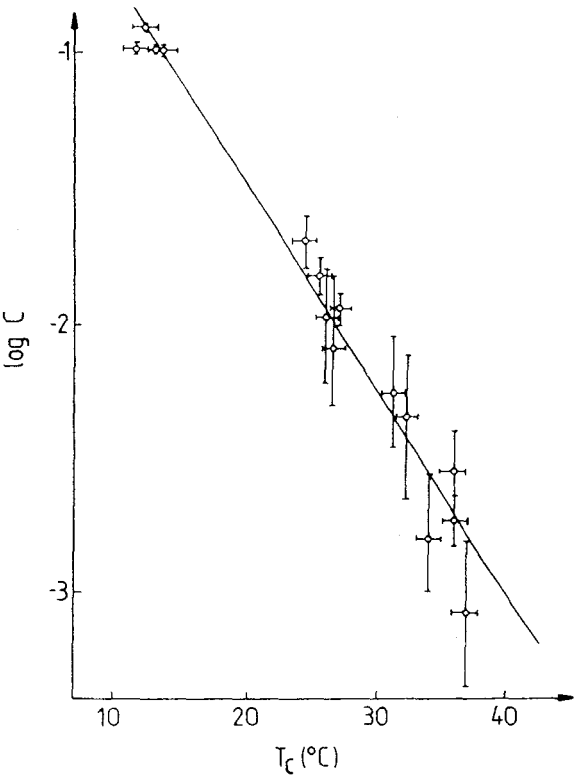


Figure 8. Logarithmic plot of the salt concentration c against the phase transition temperature, T_c. The gradient of the plot is equal to $-0.077\ K^{-1}$.

Crawford *et al.* (1991) found $\psi_0 = 70$ mV for the n-butylammonium vermiculite gels and Low (1987) found $\psi_0 = 60$ mV for the Na smectites, both results being independent of electrolyte concentration. These results invalidate the use of the Nernst equation as a first principle in colloid science, as attempted by Etelaie (1993). Understanding the non-Nernstian behaviour of these clay systems is a question of great interest in colloid science.

CONCLUSION

First, the DLVO theory cannot satisfactorily explain the raw fact that a coagulated colloid can spontaneously disperse into a solvent medium. When an n-butylammonium vermiculite crystal swells osmotically, it develops spontaneously from its primary to its secondary minimum. So the latter must represent a state of lower free energy. Secondly, the DLVO theory is based on the assumption that lyophobic sols are thermodynamically unstable (with respect to the primary minimum state). The DLVO theory is therefore refuted by the simplest possible colloid experiment in which we swell a coagulated colloid (or crystal) in a beaker of solvent, and by experiments that demonstrate the thermodynamic stability of lyophobic colloids.

https://doi.org/10.1346/CCMN.1994.0420514 Published online by Cambridge University Press

The phenomenon of osmotic swelling and the thermodynamic stability of the colloidal state have perfectly natural explanations in terms of the Coulombic attraction theory. Sogami *et al.* (1992) have shown how the counterions in the simple ionic solution between the plates begin to be absorbed onto the plates as the clay layers get closer together. This reduces Z, the charge on the plates, until X, the interplate separation, becomes equal to 2a, at which point the clay has completely coalesced and Z has fallen to zero. As Z tends to zero, U^G tends to zero and hence the negative values of U^G at large particle separations represent a state of lower free energy than the crystal plus the appropriate amount of solution. This feature of CAT is a radical improvement on DLVO theory.

Quite apart from the question of the relative depths of the primary and secondary minima, CAT yields a qualitatively different prediction for the position of the secondary minimum to that afforded by DLVO theory. It is clear from the results presented here that CAT is better adapted to explain the experimental results. Furthermore, CAT predicts the experimentally observed salt fractionation effect accurately. This subtle effect is way beyond the scope of DLVO theory, which gives insufficient consideration to the two phase region of colloid stability.

All of the experimental evidence points to the n-butylammonium vermiculite swelling being governed by the Sogami potential with the Dirichlet boundary condition. There is no possibility that the experimental results presented here could be explained by DLVO theory, which is unfortunately still common currency amongst many experimental workers in the field.

ACKNOWLEDGMENTS

One of us (M.V.S.) would like to thank the S.E.R.C. for provision of an Advanced Fellowship to support this work and to thank the ERATO Project of the Research Development Corporation of Japan for their support during its completion. We would like to express our thanks to Dave Moy for his help in producing the manuscript and to Richard Heenan for his help with the LOQ experiments.

REFERENCES

Braganza, L. F., Crawford, R. J., Smalley, M. V., and Thomas, R. K. (1990) Swelling of n-butylammonium vermiculite in water: *Clays and Clay Minerals* **38**: 90–96.

Crawford, R. J., Smalley, M. V., and Thomas, R. K. (1991) The effect of uniaxial stress on the swelling of n-butylammonium vermiculite: *Advances in Colloid and Interface Science* **34**: 537–560.

Derjaguin, B. V. and Landau, L. (1941) Theory of the stability of strongly charged lyophobic sols and of the adhesion of strongly charged particles in solutions of electrolytes: *Acta Physicochimica* **14**: 633–662.

Ettelaie, R. (1993) On the Helmholtz free energy of the highly charged double plates in an electrolyte: *Langmuir* **9**: 1888–1892.

Garrett, W. G. and Walker, G. F. (1962) Swelling of some vermiculite-organic complexes in water: in *Clays and Clay Minerals, Proc. 9th Natl. Conf.,* West Lafayette, Indiana, 1960, Ada Swinford, ed., Pergamon Press, New York, 557–567.

Hashimoto, T., Todo, A., and Kawai, H. (1978) Analysis of interparticle interference effect based upon a paracrystal model: *Polymer Journal* **10**: 521–537.

Humes, R. P. (1985) *Interparticle forces in clay minerals*: Ph.D. thesis, Oxford University, Oxford, United Kingdom, 140–153.

ISIS User Guide (1992) B. C. Boland and S. Whapham, eds., SERC, Rutherford Appleton Laboratory, Report RAL 92-041.

Klaarenbeek, F. W. (1946) Over Donnan-even wichten bij solen van arabische gom: Ph.D. thesis, Utrecht.

Low, P. F. (1987) Structural component of the swelling pressure of clays: *Langmuir* **3**: 18–25.

Moody, K. R. (1992) Swelling of vermiculite-organic complexes in water: Part II thesis, Oxford University, Oxford, U.K., 26–29.

Norrish, K. and Rausell-Colom, J. A. (1963) Low angle X-ray diffraction studies of the swelling of montmorillonite and vermiculite: in *Clays and Clay Minerals, Proc. 10th Natl. Conf.,* Austin, Texas, 1961, Ada Swinford and P. C. Franks, eds., Pergamon Press, New York, 123–149.

Rausel-Colom, J. A. (1964) Small-angle X-ray diffraction study of the swelling of butylammonium vermiculite: *Trans. Far. Soc.* **60**: 190–201.

Rausell-Colom, J. A., Saez-Aunon, J., and Pons, C. H. (1989) Vermiculite gelation: Structural and textural evolution: *Clay Miner.* **24**: 459–478.

Smalley, M. V. (1990) Electrical interaction in macroionic solutions and gels: *Molecular Physics* **71**: 1251–1267.

Smalley, M. V. (1994) Electrostatic theory of clay swelling: *Langmuir,* to be published.

Smalley, M. V., Thomas, R. K., Braganza, L. F., and Matsuo, T. (1989) Effect of hydrostatic pressure on the swelling of n-butylammonium vermiculite: *Clays and Clay Minerals* **37**: 474–478.

Sogami, I. (1983) Effective potential between charged spherical particles in dilute suspension: *Phys. Lett.* **96A,** 199–203.

Sogami, I. and Ise, N. (1984) On the electrostatic interaction in macroionic solutions: *J. Chem. Phys.* **81**: 6320–6332.

Sogami, I. S., Shinohara, T., and Smalley, M. V. (1991) Effective interaction of highly charged plates in an electrolyte: *Molecular Physics* **74**: 599–612.

Sogami, I. S., Shinohara, T., and Smalley, M. V. (1992) Adiabatic pair potential of highly charged plates in an electrolyte: *Molecular Physics* **76**: 1–19.

Townshend, D. J. (1992) Vermiculite gelation: Part II thesis, Oxford University, Oxford, U.K., 13–24.

Verwey, E. J. W. and Overbeek, J. Th. G. (1948) Theory of the stability of lyophobic colloids: Elsevier, Amsterdam.

Walker, G. F. (1960) Macroscopic swelling of vermiculite crystals in water: *Nature* **187**: 312–313.

(Received 20 September 1993; accepted 18 March 1994; Ms. 2418)

https://doi.org/10.1346/CCMN.1994.0420514 Published online by Cambridge University Press